Article:
Kusins, J., Knowles, N., Ryan, M. et al. (2 more authors) (2020) Full-field comparisons between strains predicted by QCT-derived finite element models of the scapula and experimental strains measured by digital volume correlation. Journal of Biomechanics, 113. 110101. ISSN 0021-9290

https://doi.org/10.1016/j.jbiomech.2020.110101

Journal of Biomechanics 113 (2020) 110101

Contents lists available at ScienceDirect

Journal of Biomechanics

journal homepage: www.elsevier.com/locate/jbiomech
www.JBiomech.com

Full-field comparisons between strains predicted by QCT-derived finite element models of the scapula and experimental strains measured by digital volume correlation

Jonathan Kusins [a,b], Nikolas Knowles [c], Melissa Ryan [d], Enrico Dall'Ara [d], Louis Ferreira [a,b,*]

[a] Department of Mechanical and Materials Engineering, Western University, London, Ontario, Canada
[b] Roth|McFarlane Hand and Upper Limb Centre, St. Joseph's Health Care, London, Ontario, Canada
[c] Department of Radiology, Cumming School of Medicine, University of Calgary, Calgary, Alberta, Canada
[d] Department of Oncology and Metabolism and Insigneo:Institute for In Silico Medicine, University of Sheffield, Sheffield, UK

ARTICLE INFO

Article history:
Accepted 12 October 2020

Keywords:
Subject-specific finite element analysis
Digital volume correlation
Shoulder FEM
CT-compatible loading

ABSTRACT

Subject-specific finite element models (FEMs) of the shoulder can be used to evaluate joint replacement designs preclinically. However, to ensure accurate conclusions are drawn, experimental validation is critical. The objective of the current study was to evaluate the accuracy of strain predictions generated by subject-specific scapula FEMs through comparisons against full-field experimental strains measured using digital volume correlation (DVC). Three cadaveric scapulae were mechanically loaded using a custom-hexapod robot within a micro-CT scanner. BoneDVC was used to quantify resultant experimental full-field strains. Scapula FEMs were generated using three different density-modulus relationships to assign material properties. Two types of boundary conditions (BCs) were simulated: DVC-displacement-driven or applied-force-driven. Third principal strains were compared between the DVC measurements and FEM predictions. With applied-force BCs, poor agreement was observed between the predicted and measured strains (slope range: 0.16–0.19, r^2 range: 0.04–0.30). Agreement was improved with the use of DVC-displacement BCs (slope range: 0.54–0.59, r^2 range: 0.73–0.75). Strain predictions were independent of the density-modulus relationship used for DVC-displacement BCs, but differences were observed in the correlation coefficient and intercept for applied-force BCs. Overall, this study utilized full-field DVC-derived experimental strains for comparison with FEM predicted strains in models with varying material properties and BCs. It was found that fair agreement can be achieved in localized strain measurements between DVC measurements and FEM predictions when DVC-displacement BCs are used. However, performance suffered with use of applied-force BCs.

1. Introduction

Subject-specific finite element models (FEM) of the shoulder offer the capability to evaluate the performance of joint replacement designs prior to clinical adoption (Geraldes et al., 2017). As these models can isolate and alter design variables in a cost-effective and parametric fashion, they offer distinct advantages over experimental bench-top testing. However, simplifying assumptions can influence the predicted outcomes. For strain-based outcomes, the assignment of material properties using density-modulus relationships and simulated boundary conditions are cited sources of variability (Helgason et al., 2016; Hussein et al., 2018). Therefore, experimental validation should be performed whenever possible to ensure the fidelity of the FEM.

In-vitro biomechanical testing has previously been conducted to assess the accuracy of subject-specific shoulder FEMs in predicting strain-based outcomes (Dahan et al., 2019, 2016). To quantify strain, a common experimental method includes the use of a strain gauge which is adhered to the surface of a cadaveric specimen (Grassi and Isaksson, 2015). However, as strain gauges only provide a discrete surface measurement, they do not offer insight into the mechanical strain distribution beneath the cortical shell. Recently, mechanical testing combined with high-resolution computed tomography (CT) and digital volume correlation (DVC) algorithms have been used to measure full-field strains throughout the structure of bone and has previously been applied to the shoulder (Kusins et al., 2019; Zhou et al., 2020). DVC has also been applied to

* Corresponding author at: Roth|McFarlane Hand and Upper Limb Centre, Surgical Mechatronics Laboratory, St. Josephs Health Care, 268 Grosvenor St., London, ON, Canada.
E-mail address: lferreir@uwo.ca (L. Ferreira).

https://doi.org/10.1016/j.jbiomech.2020.110101
0021-9290/

other bones such as the vertebra (Costa et al., 2017; Jackman et al., 2016; Tozzi et al., 2016) and femur (Rapagna et al., 2019; Ridzwan et al., 2017) and has previously been used as an experimental benchmark for comparison to full-field predictions of whole bone FEMs (Jackman et al., 2016; Kusins et al., 2020; Oliviero et al., 2018).

The objective of the current study was to quantify the accuracy of subject-specific FEMs of the scapula in predicting experimental full-field strains obtained from an *in-vitro* mechanical testing protocol. Two factors in the generation of subject-specific FEMs were evaluated: (1) three different density-modulus equations used for material property assignment and (2) two types of simulated boundary conditions.

2. Methods

2.1. Specimen acquisition and experimental testing

Three fresh-frozen cadaveric arms were used for experimental testing (Table 1). Each arm was scanned using a clinical QCT-scanner (GE Discovery CT750 HD, Milwaukee, WI, USA) at clinical settings (pixel size: 0.625–0.668 mm, slice thickness: 0.625 mm, 120 kVp, 200 mA, BONEPLUS) with a dipotassium phosphate (K_2HPO_4) calibration phantom as detailed in a previous study (Knowles et al., 2019; Kusins et al., 2019). Following the scanning protocol, the scapula was removed, denuded of all soft tissues, and potted in polymethyl methacrylate (PMMA). The articular surface of the glenoid was then resurfaced using a surgical shoulder arthroplasty reamer to ensure a uniform surface for experimental loading.

The experimental testing protocol used within the current study has previously been detailed (Knowles et al., 2019; Kusins et al., 2019) and is briefly discussed here. A CT-compatible loading device was used to apply an external load to the cadaveric scapulae (Fig. 1) measured by a load cell (Mini 45, ATI Industrial Automation, NC, USA). Experimental loading was performed on each specimen within a cone-beam micro-CT scanner (Nikon XT H 225 ST, Nikon Metrology, NV). A hemispherical platen (48 mm diameter, Delrin®) transferred loads from the loading device to the articular surface of the specimen. A pre-loaded micro-CT scan (33.5 μm isotropic voxels, 95 kVp, 64 μA, 3141 projections, 1000 ms exposure) was acquired with an applied pre-load of 10 N. A target 500 N compressive load was then applied using the loading device within the micro-CT scanner. For one cadaveric scapula, two pre-loaded scans were acquired to quantify the accuracy and precision of the strain measurements using a standard procedure that compares two undeformed images and assumes a zero-strain condition (Dall'Ara et al., 2014; Liu and Morgan, 2007). A settling time of 20 min was allowed for tissue relaxation prior to acquiring the post-loaded micro-CT scan with similar imaging settings to the pre-loaded scan.

2.2. Strain measurements

BoneDVC (https://bonedvc.insigneo.org/dvc/) was used to quantify full-field local displacements and strains by registering the micro-CT images of the pre- and post-loaded specimen

Table 1
Specimen demographics.

	Gender	Age (Years)
Specimen 1	Male	73
Specimen 2	Female	62
Specimen 3	Female	52

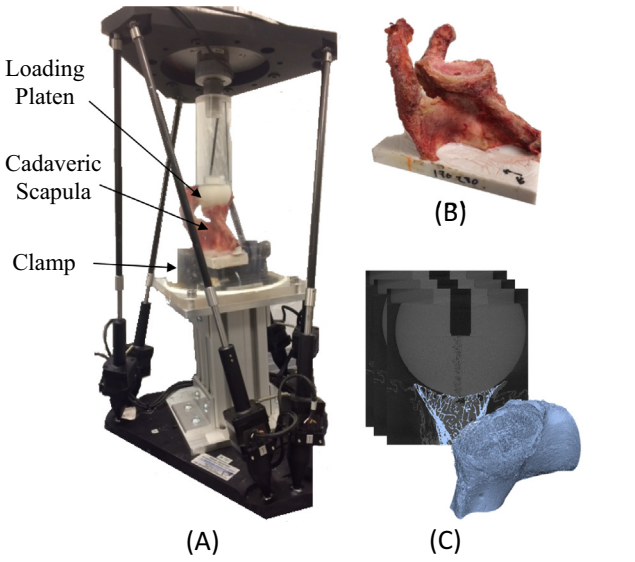

Fig. 1. (A) Compressive loading was performed within a micro-CT scanner using a custom-made CT-compatible loading device. The cadaveric scapula (B) was denuded of all soft-tissue for simultaneous experimental loading and micro-CT imaging (C).

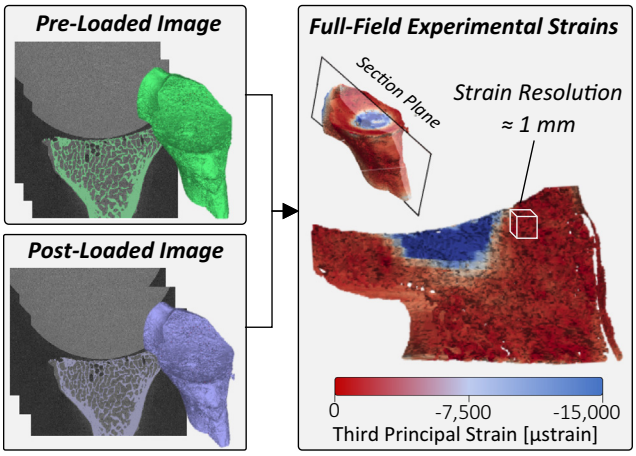

Fig. 2. Full-field experimental strains (resolution ≈ 1 mm) between pre- and post-loaded micro-CT images (33.5 μm) were calculated using BoneDVC.

(Fig. 2). BoneDVC is a global DVC software based on a combination of elastic registration to compute the displacements and differentiation with a finite element software for calculating the strains. The underlying algorithms have previously been reported in details (Dall'Ara et al., 2017, 2014). Prior to performing the DVC registrations, pre-processing of the images was conducted. A mask that contained only scapula bone was obtained through segmentation of the micro-CT images. Any voxels outside of the mask were set to a constant value. The images were then converted to 8-bit binary for the DVC registrations. To determine the optimal spatial resolution of BoneDVC, a standard procedure of comparing two unloaded scans (known zero-strain case (Liu and Morgan, 2007)) was performed to assess the accuracy and precision of the resultant strain measurements. Based on these results, a distance between two measurements of displacement (nodal spacing) of 30 was found to provide the best compromise between spatial resolution (≈ 1 mm) and experimental uncertainties (strain accuracy equal to 220 μstrain and strain precision equal to 366 μstrain).

2.3. Finite element model generation

Scapula FEMs were generated for each specimen using the previously acquired clinical QCT scans. The rationale of using QCT scans to generate the FEMs was to use a clinically feasible imaging technique for model generation and to be consistent with previous scapula FE modelling approaches (Zheng et al., 2017). For each scapula, the geometry was extracted using a global threshold segmentation and filled using Mimics software (Mimics v.20.0, Materialise, Leuven, BE). To identify bone that was removed during specimen preparation, a hand-held surface scanner (Spider, Artec 3D, Luxembourg) was used to generate STL surface models of the scapulae. The models were co-registered using an iterative closest point registration (3-matic v.12.0, Materialise, Leuven, BE) and any bone removed during specimen preparation was virtually removed via Boolean subtraction.

To assign material properties to the FEMs, a quadratic tetrahedral (edge length = 1 mm) mesh was generated using Abaqus (v.6.14, Simulia, Providence, RI). Three separate FEMs with varying material properties were created using specimen-specific densiometric calibrations and three different density-modulus relationships (Table 2).

Two types of boundary conditions (BCs) were simulated: DVC-displacement-driven and applied-force-driven. DVC-displacement BCs consisted of applying local DVC experimental displacements to the articular surface and medial surface of the scapula FEM (Fig. 3) (Chen et al., 2017; Kusins et al., 2019). A custom-code (Matlab v.R2019a, Natick, MA) was used to tri-linear interpolate local displacements in the Cartesian directions from the DVC results to the nodes of the FEM. Applied-force BCs consisted of applying the experimentally measured force to a virtual loading platen. The virtual loading platen was meshed with hexahedral elements (E = 3100 MPa, ν = 0.35) and contact between the loading platen and virtual scapula was simulated (Kusins et al., 2019). To isolate the load transfer at the platen-scapula interface, DVC-displacements were assigned to the medial aspect of the virtual scapula (Fig. 3).

Table 2
Density-modulus equations used for FEM material assignment.

Equation	Density-modulus relationship	
1	[a] $E = 32790 * \rho_{qct}^{2.307}$	
2	[b] $E = 15000 * \left(\frac{\rho_{app}}{1.8}\right)^2$	
3	Density range	Density-modulus elationship
	$\rho_{app} < 1.54 g/cm^3$	[c] $E_{trab} = 60 + 900 * \rho_{app}^2$
	$\rho_{app} \geq 1.54 g/cm^3$	[d] $E_{cort} = 90 * \rho_{app}^{7.4}$

Density-modulus relationships are from:
[a] Knowles et al. (2019b).
[b] Büchler et al. (2002).
[c] Schaffler and Burr (1988).
[d] Rice et al. (1988). E in [MPa], ρ_{qct} in [gK_{2HPO4}/cm^3] and ρ_{app} in [g/cm^3].

2.4. Statistical analysis

To compare third principal strains predicted by the scapula FEM to the experimental strains measured by DVC, regions of interest (ROI) throughout the glenoid vault were defined. Four depth ROIs were created, divided into four volumes of equal depth (1 mm thick). The first depth ROI (depth 1) was located 1.5 mm below the articular surface of the glenoid. Each depth ROI was further subdivided into four concentric rings centered about the reamed pilot hole (diameter = 8 mm). The inner diameter of the most central ring (radius 1) was equal to the outer diameter of the pilot hole and the remaining rings were spaced peripherally by 2.5 mm but constrained by the geometry of the scapula. In total, 16 ROIs were included within the glenoid vault. The average value of third principal strain within each ROI of the FE models were compared with the DVC results using linear regression analyses. Slope and intercept of the regressions were compared using an analysis of covariance (ANCOVA) with $\alpha = 0.05$. Within each ROI, root-mean-square error (RMSE) was also calculated by comparing region-averaged FEM strains to corresponding DVC experimental strain measurements. RMSE% was calculated by dividing the RMSE by the maximum experimental strain measurement for each specimen.

3. Results

The accuracy of strains predicted by the FEM was impacted by the BC simulated. For the pooled results, DVC-displacement BCs (slope range: 0.54–0.59, r^2 range: 0.73–0.75) was found to improve strain predictions compared to applied-force BCs (slope range:

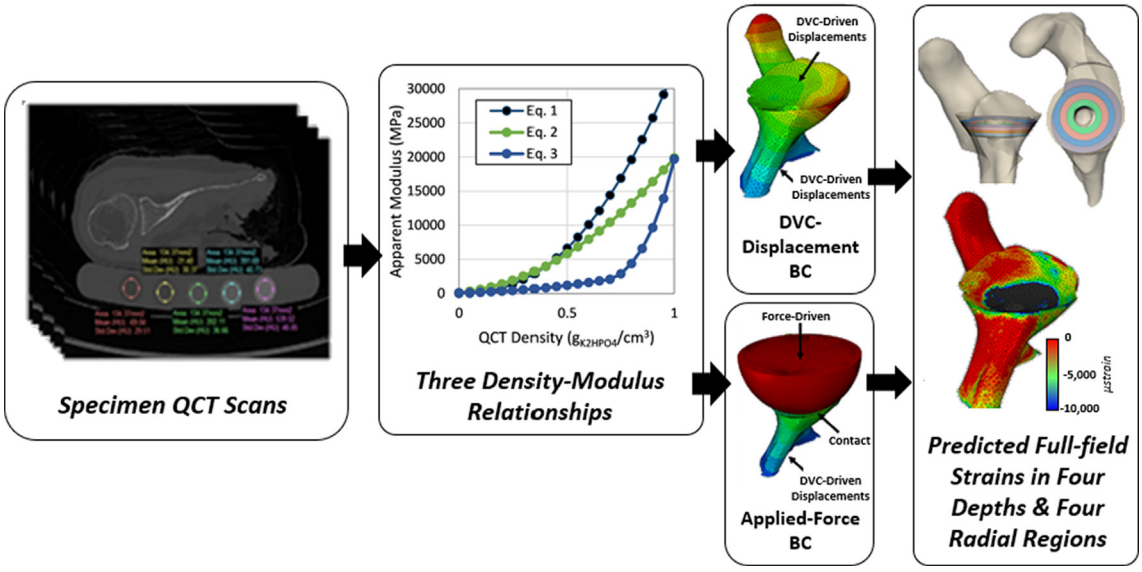

Fig. 3. Finite element models of the scapula were generated from clinical QCT scans. Three separate density-modulus equations were used to assign material properties to the finite element model. Two separate boundary conditions (DVC-displacement and applied-force) were simulated.

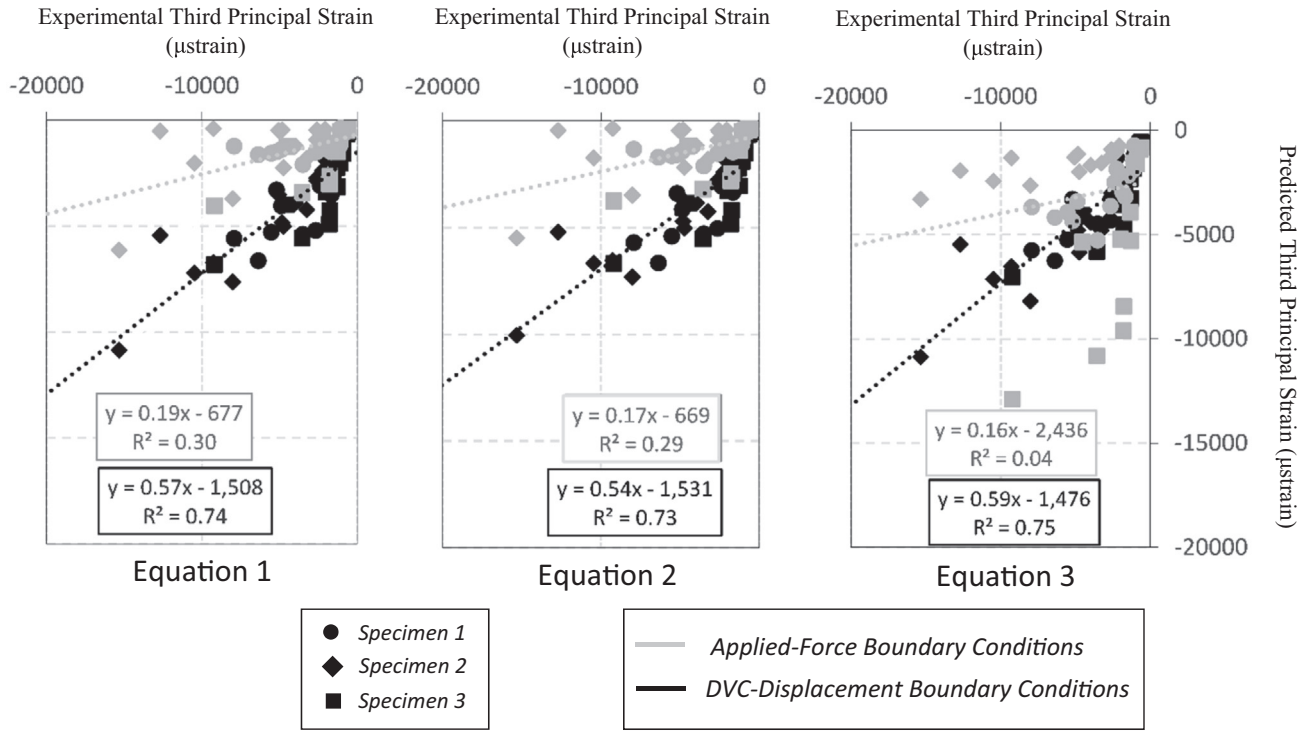

Fig. 4. Pooled linear correlation results comparing experimental strains measured using DVC to predicted FEM strains. The results of the FEM with three separate density-modulus equations are shown. As well, two types of boundary conditions were simulated for each FEM: applied-force (grey) and DVC-displacement (black).

0.16–0.19, r^2 range: 0.04–0.30) (Fig. 4) with differences in slope ($p < 0.001$) for all three density-modulus equations. For models with DVC-displacement BCs, varying the density-modulus equation did not alter the agreement with the experimental measurements (no significant differences for slope or intercept were present between the models ($p > 0.05$)). Colour maps of each specimen depicting the experimental DVC strains and the FEM predicted strains with density-modulus equation three and both types of BCs are shown in Fig. 5. For each specimen, coefficient of correlation was improved with the use of DVC-displacement BCs (r^2 range: 0.63–0.79) compared to applied-force BCs (r^2 range: 0.50–0.66) (Table 3).

Highest errors associated with strain predictions of the FEM were found within the ROI closest to the loading platen (depth 1, radius 1) and this was consistent for all FEMs (Fig. 6). Within this ROI, higher errors were observed with the use of applied-force BCs (RMSE% of 31.9–33.1%) compared to DVC-displacement BCs (RMSE% of 19.3–21.3%). When considering all ROIs together, lower

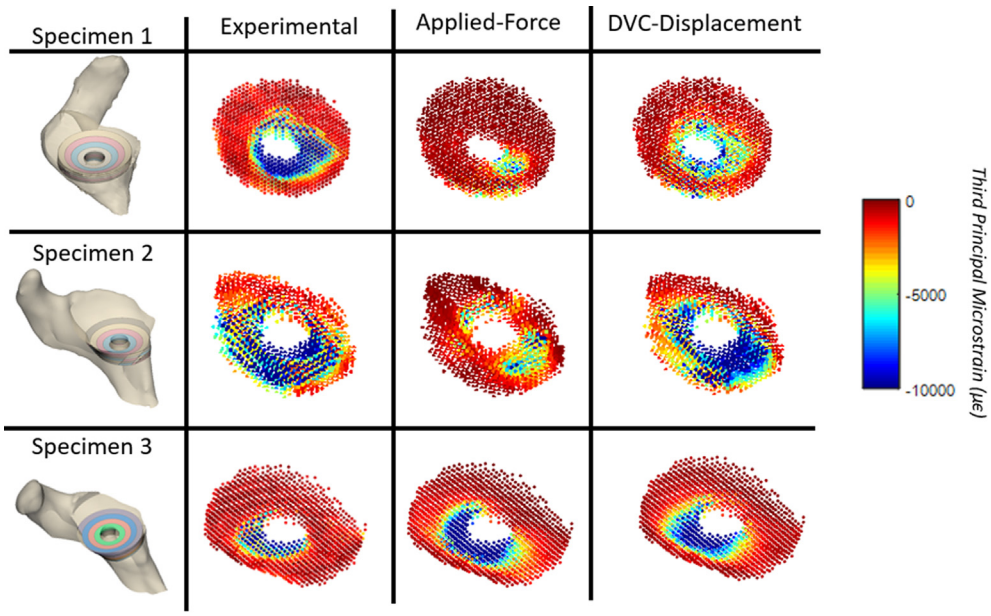

Fig. 5. Colour maps of experimental third principal strain fields as measured by DVC compared to FEM predicted strains using density-modulus equation 3 with applied-force or DVC-displacement BCs. All ROIs (depth and radius) are included within the colour maps.

Table 3
Linear regression results comparing experimental DVC and predicted FEM strains.

Specimen #	DVC-displacement BCs		Applied-force BCs	
	Slope (m)	Coefficient of Correlation (r^2)	Slope (m)	Coefficient of Correlation (r^2)
1	0.72	0.79	0.40	0.50
2	0.49	0.76	0.14	0.66
3	0.75	0.63	1.39	0.59

Predicted strains compared from FEMs were simulated using density-modulus relationship 3.

errors were present in FEMs with DVC-displacement BCs (RMSE% between 10.1% and 11.3%) compared to applied-force BCs (RMSE % between 13.3% and 17.0%).

4. Discussion

The objective of this study was to evaluate the accuracy of full-field strains predicted by scapula FEMs compared to experimentally measured DVC strains. The strains predicted by the FEMs were found to be sensitive to the BC simulated. Within this study, DVC-displacement-driven BCs (r^2 between 0.73 and 0.75) was found to improve the accuracy of full-field strains predicted by the FEM compared to applied-force-driven BCs (r^2 between 0.04 and 0.30). This result highlights the importance of reproducing accurately the FEM's BCs in validation studies as reported also for micro-FEMs of trabecular bone (Chen et al., 2017). For DVC-displacement BCs, the FEMs generally underpredicted the experimental strains as indicated by a slope less than 1. Highest errors for each FEM occurred within the ROI closest to the loading platen. Within this region, high experimental strains were also measured (>10,000 μstrain) which may indicate that local experimental plastic deformation of the trabecular bone occurred (Bayraktar et al., 2004). Material non-linearity was not accounted for within the FEMs as material properties were assumed to be linear isotropic (Zheng et al., 2017) and this may have affected the accuracy of strains predicted within this study. As strains are often used as a surrogate measure for bone remodeling algorithms to assess implant longevity (Comenda et al., 2019), implementing local yielding criteria for scapula FEMs warrants further investigation.

A validated FEM with force-controlled BCs is desirable as it can be extrapolated outside the experimental conditions. The applied-force BCs simulated within the current study resulted in poor agreement regardless of the material property equation used. Although the placement of the loading platen was extracted from the microCT images, the FEMs' strain patterns observed with applied-force BCs disagreed with the experimental results. This may be attributed to the contact constraints imposed within the FEMs but also the material properties that were assigned to the scapula FEMs. We found that the agreement between the predicted and experimental strains of the pooled results improved with the use of either density-modulus relationship 1 or 2 compared to relationship 3; however, overall poor agreement was observed regardless of the relationship used (r^2 less than 0.35) when using applied-force BCs. Evidently, further refinement is required before the model can be considered experimentally validated. However, this finding demonstrates the strength of using DVC as an experimental validation tool, as it provides the capability to quantify internal strains throughout the glenoid vault and allows for a full-field validation assessment that would not be possible with traditional surface-based strain measurement tools (Grassi and Isaksson, 2015).

There were limitations with this study. First, a low sample size (n = 3) of specimens was tested. As well, strains were compared within volumetric ROIs rather than a full-field point by point validation. It should be noted that by region-averaging strains, the pooled linear regression results within the current study are more indicative of whether the FEM can replicate the overall pattern of strain rather than predictions at discrete continuous locations throughout the trabecular structure. This in turn limits the overall strain spatial resolution of our validation procedure. In order to resolve strains at the trabecular level, combining mechanical loading techniques with volumetric imaging at the nano scale would be required (Comini et al., 2019; Kersh, 2020).

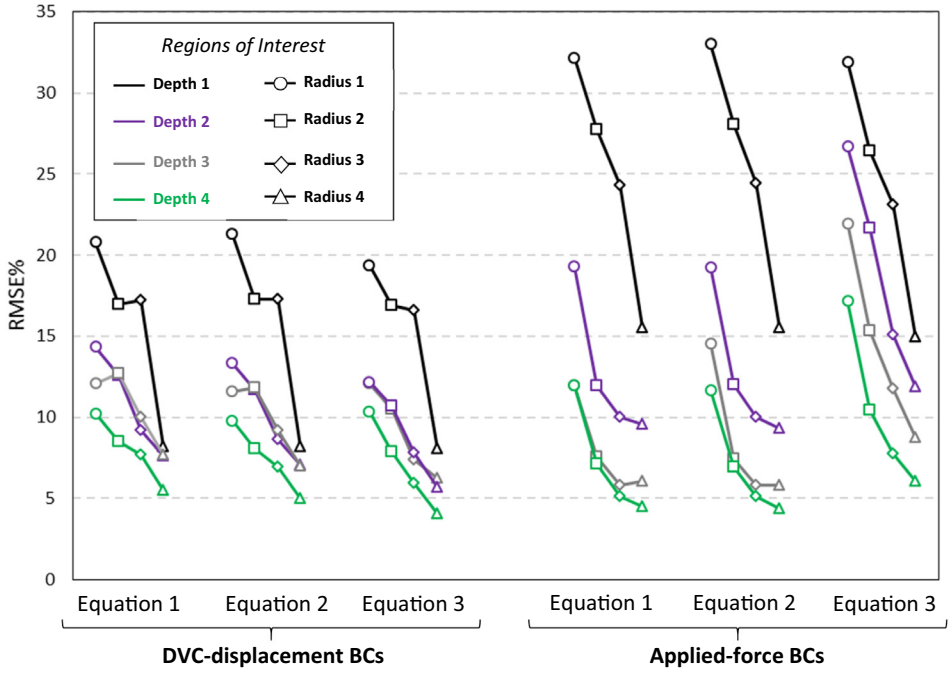

Fig. 6. Average RMSE% (n = 3) for predicted FEM strains as a function of density-modulus equations and boundary conditions (BCs).

Overall, this study builds upon previous work in validating full-field displacements and global reaction forces obtained for scapula FEMs (Knowles et al., 2019; Kusins et al., 2019). Consistent with previous work, the use of DVC-displacement-driven BCs was found to improve the full-field predictions of scapula FEMs. Continual development of modelling approaches in conjunction with DVC should continue to improve the clinical translatability of FEMs of the scapula.

Declaration of Competing Interest

The authors declare that they have no known competing financial interests or personal relationships that could have appeared to influence the work reported in this paper.

Acknowledgements

Funding was provided by the Natural Sciences and Engineering Research Council (NSERC), [funding reference number: RGPIN/418656]. Jonathan Kusins is supported in part by a Post Graduate Scholarship from the Natural Sciences and Engineering Research Council and a Transdisciplinary Bone & Joint Training Award from the Collaborative Training Program in Musculoskeletal Health Research at Western University. Nikolas Knowles is a Canadian Institutes of Health Research (CIHR) Banting Postdoctoral Fellow. The BoneDVC approach was developed under projects funded by the Engineering and Physical Sciences Research Council (Grant numbers: EP/K03877X/1, EP/S032940/1, and EP/P015778/1).

References

Bayraktar, H.H., Morgan, E.F., Niebur, G.L., Morris, G.E., Wong, E.K., Keaveny, T.M., 2004. Comparison of the elastic and yield properties of human femoral trabecular and cortical bone tissue. J. Biomech. 37, 27–35. https://doi.org/10.1016/S0021-9290(03)00257-4.

Büchler, P., Ramaniraka, N.A., Rakotomanana, L.R., Iannotti, J.P., Farron, A., 2002. A finite element model of the shoulder: application to the comparison of normal and osteoarthritic joints. Clin. Biomech. (Bristol, Avon) 17, 630–639. https://doi.org/10.1016/S0268-0033(02)00106-7.

Chen, Y., Dall'Ara, E., Sales, E., Manda, K., Wallace, R., Pankaj, P., Viceconti, M., 2017. Micro-CT based finite element models of cancellous bone predict accurately displacement once the boundary condition is well replicated: a validation study. J. Mech. Behav. Biomed. Mater. 65, 644–651. https://doi.org/10.1016/j.jmbbm.2016.09.014.

Comenda, M., Quental, C., Folgado, J., Sarmento, M., Monteiro, J., 2019. Bone adaptation impact of stemless shoulder implants: a computational analysis. J. Shoulder Elbow Surg. 28, 1886–1896. https://doi.org/10.1016/j.jse.2019.03.007.

Comini, F., Palanca, M., Cristofolini, L., Dall'Ara, E., 2019. Uncertainties of synchrotron microCT-based digital volume correlation bone strain measurements under simulated deformation. J. Biomech. 86, 232–237. https://doi.org/10.1016/j.jbiomech.2019.01.041.

Costa, M.C., Tozzi, G., Cristofolini, L., Danesi, V., Viceconti, M., Dall'Ara, E., 2017. Micro Finite Element models of the vertebral body: validation of local displacement predictions. Plos One 12, 1–18. https://doi.org/10.1371/journal.pone.0180151.

Dahan, G., Trabelsi, N., Safran, O., Yosibash, Z., 2019. Finite element analyses for predicting anatomical neck fractures in the proximal humerus. Clin. Biomech. 68, 114–121. https://doi.org/10.1016/j.clinbiomech.2019.05.028.

Dahan, G., Trabelsi, N., Safran, O., Yosibash, Z., 2016. Verified and validated finite element analyses of humeri. J. Biomech. 49, 1094–1102. https://doi.org/10.1016/j.jbiomech.2016.02.036.

Dall'Ara, E., Barber, D., Viceconti, M., 2014. About the inevitable compromise between spatial resolution and accuracy of strain measurement for bone tissue: a 3D zero-strain study. J. Biomech. 47, 2956–2963. https://doi.org/10.1016/j.jbiomech.2014.07.019.

Dall'Ara, E., Peña-Fernández, M., Palanca, M., Giorgi, M., Cristofolini, L., Tozzi, G., 2017. Precision of digital volume correlation approaches for strain analysis in bone imaged with micro-computed tomography at different dimensional levels. Front. Mater. 4. https://doi.org/10.3389/fmats.2017.00031.

Geraldes, D.M., Hansen, U., Amis, A.A., 2017. Parametric analysis of glenoid implant design and fixation type. J. Orthop. Res. 35, 775–784. https://doi.org/10.1002/jor.23309.

Grassi, L., Isaksson, H., 2015. Extracting accurate strain measurements in bone mechanics: a critical review of current methods. J. Mech. Behav. Biomed. Mater. 50, 43–54. https://doi.org/10.1016/j.jmbbm.2015.06.006.

Helgason, B., Gilchrist, S., Ariza, O., Vogt, P., Enns-Bray, W., Widmer, R.P., Fitze, T., Pálsson, H., Pauchard, Y., Guy, P., Ferguson, S.J., Cripton, P.A., 2016. The influence of the modulus–density relationship and the material mapping method on the simulated mechanical response of the proximal femur in side-ways fall loading configuration. Med. Eng. Phys. 38, 679–689. https://doi.org/10.1016/j.medengphy.2016.03.006.

Hussein, A.I., Louzeiro, D.T., Unnikrishnan, G.U., Morgan, E.F., 2018. Differences in trabecular microarchitecture and simplified boundary conditions limit the accuracy of quantitative computed tomography-based finite element models of vertebral failure. J. Biomech. Eng. 140, 1–11. https://doi.org/10.1115/1.4038609.

Jackman, T.M., DelMonaco, A.M., Morgan, E.F., 2016. Accuracy of finite element analyses of CT scans in predictions of vertebral failure patterns under axial compression and anterior flexion. J. Biomech. 49, 267–275. https://doi.org/10.1016/j.jbiomech.2015.12.004.

Kersh, M.E., 2020. Resolving nanoscale strains in whole joints. Nat. Biomed. Eng. 4, 257–258. https://doi.org/10.1038/s41551-020-0531-z.

Knowles, N.K., Kusins, J., Faieghi, M., Ryan, M., Dall'Ara, E., Ferreira, L.M., 2019a. Material mapping of QCT-derived scapular models: a comparison with micro-CT loaded specimens using digital volume correlation. Ann. Biomed. Eng. 47, 2188–2198. https://doi.org/10.1007/s10439-019-02312-2.

Knowles, N.K., Langohr, G.D.G., Faieghi, M., Nelson, A., Ferreira, L., 2019b. Development of a validated glenoid trabecular density-modulus relationship. J. Mech. Behav. Biomed. Mater. 90, 140–145. https://doi.org/10.1016/j.jmbbm.2018.10.013.

Kusins, J., Knowles, N., Columbus, M., Oliviero, S., Dall'Ara, E., Athwal, G.S., Ferreira, L.M., 2020. The application of digital volume correlation (DVC) to evaluate strain predictions generated by finite element models of the osteoarthritic humeral head. Ann. Biomed. Eng. https://doi.org/10.1007/s10439-020-02549-2

Kusins, J., Knowles, N., Ryan, M., Dall'Ara, E., Ferreira, L., 2019. Performance of QCT-Derived scapula finite element models in predicting local displacements using digital volume correlation. J. Mech. Behav. Biomed. Mater. 97, 339–345. https://doi.org/10.1016/j.jmbbm.2019.05.021.

Liu, L., Morgan, E.F., 2007. Accuracy and precision of digital volume correlation in quantifying displacements and strains in trabecular bone. J. Biomech. 40, 3516–3520. https://doi.org/10.1016/j.jbiomech.2007.04.019.

Oliviero, S., Giorgi, M., Dall'Ara, E., 2018. Validation of finite element models of the mouse tibia using digital volume correlation. J. Mech. Behav. Biomed. Mater. 86, 172–184. https://doi.org/10.1016/j.jmbbm.2018.06.022.

Rapagna, S., Berahmani, S., Wyers, C.E., van den Bergh, J.P.W., Reynolds, K.J., Tozzi, G., Janssen, D., Perilli, E., 2019. Quantification of human bone microarchitecture damage in press-fit femoral knee implantation using HR-pQCT and digital volume correlation. J. Mech. Behav. Biomed. Mater. 97, 278–287. https://doi.org/10.1016/j.jmbbm.2019.04.054.

Rice, J., Cowin, S., Bowman, J., 1988. On the dependence of the elasticity and strength of cancellous bone on apparent density. J. Biomech.

Ridzwan, M.I.Z., Sukjamsri, C., Pal, B., van Arkel, R.J., Bell, A., Khanna, M., Baskaradas, A., Abel, R., Boughton, O., Cobb, J., Hansen, U.N., 2017. Femoral fracture type can be predicted from femoral structure: A finite element study validated by digital volume correlation experiments. J. Orthop. Res. 993–1001. https://doi.org/10.1002/jor.23669.

Schaffler, M., Burr, D., 1988. Stiffness of compact bone: effects of porosity and density. J. Biomech.

Tozzi, G., Danesi, V., Palanca, M., Cristofolini, L., 2016. Elastic full-field strain analysis and microdamage progression in the vertebral body from digital volume correlation: strain analysis in the vertebral body from digital volume correlation. Strain 52, 446–455. https://doi.org/10.1111/str.12202.

Zheng, M., Zou, Z., Bartolo, P.J.D.S., Peach, C., Ren, L., 2017. Finite element models of the human shoulder complex: a review of their clinical implications and modelling techniques: finite element models of human shoulder complex. Int. J. Numer. Meth. Biomed. Engng. 33, e02777. https://doi.org/10.1002/cnm.2777.

Zhou, Y., Gong, C., Lewis, G.S., Armstrong, A.D., Du, J., 2020. 3D full-field biomechanical testing of a glenoid before and after implant placement. Extreme Mech. Lett. 35. https://doi.org/10.1016/j.eml.2019.100614.